Pergamon

SCIENCE DIRECT®

Bioorganic & Medicinal Chemistry 11 (2003) 3121–3132

BIOORGANIC & MEDICINAL CHEMISTRY

Synthesis and Testing of Novel Classical Cannabinoids: Exploring the Side Chain Ligand Binding Pocket of the CB1 and CB2 Receptors

Asha K. Nadipuram,[a] Mathangi Krishnamurthy,[a] Antonio M. Ferreira,[b] Wei Li[a] and Bob M. Moore, II[a,*]

[a]*Department of Pharmaceutical Sciences, College of Pharmacy, University of Tennessee-Memphis, Memphis, TN 38103, USA*

[b]*Computational Research on Materials Institute, Department of Chemistry, University of Memphis, Memphis, TN 38152, USA*

Received 24 January 2003; revised 4 April 2003; accepted 7 April 2003

Abstract—A series of C3 cyclic side-chain analogues of classical cannabinoids were synthesized to probe the ligand binding pocket of the CB1 and CB2 receptors. The analogues were evaluated for CB1 and CB2 receptor binding affinities relative to Δ^8-THC. The C3 side-chain geometries of the analogues were studied using high field NMR spectroscopy and quantum mechanical calculations. The results of these studies provide insights into the geometry of the ligand binding pocket of the CB1 and CB2 receptors.

Introduction

Delta-9-tetrahydrocannabinol (Δ^9-THC) was isolated and identified as the major active constituent of marijuana in 1964 by Mechoulam and coworkers.[1] In the following decades, the CB1 and CB2 receptors were discovered, characterized and shown to be responsible for the actions of Δ^9-THC.[2-5] The CB1 and CB2 receptors have since gained attention as potential therapeutic targets for the development of antiobesity,[6] anticancer,[7] analgesic,[8] and antiglaucoma agents.[9,10] Efforts to develop therapeutic agents have resulted in the identification of a number of structurally distinct classes of compounds that bind to the cannabinoid receptors, these include the classical cannabinoids (Δ^9-THC, **1**), the non-classical cannabinoids (CP55,940, **2**),[11] the diarylpyrazoles (AM-251, **3**),[12] and aminoalkylindoles (WIN-55212, **4**).[13] By far the most extensively studied cannabinoid analogues in terms of the pharmacology and SAR are the classical and non-classical cannabinoids.

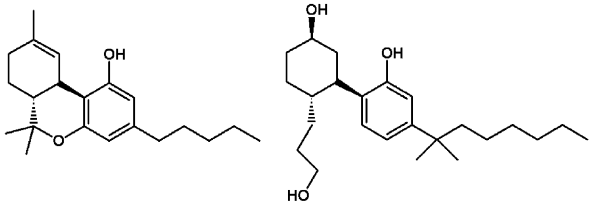

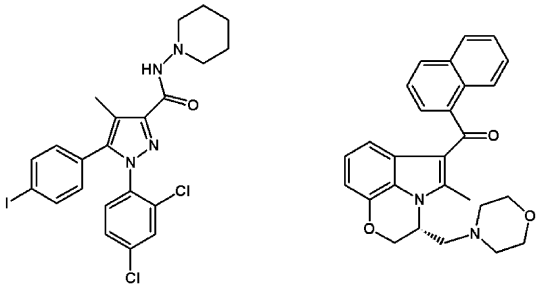

The binding affinity of the classical cannabinoids (CCBs) and non-classical cannabinoids to the CB1 receptor can generally be defined in terms of a three point and four point pharmacophore model, respectively.[14]

*Corresponding author. Tel.: +1-909-448-6085; fax: +1-901-448-6828; e-mail: bmoore@utmem.edu

0968-0896/03/$ - see front matter © 2003 Elsevier Science Ltd. All rights reserved.
doi:10.1016/S0968-0896(03)00238-4

The structural elements that comprise the three point pharmacophore of the CCB analogues are: (1) a phenolic group in the C1 position of the aromatic ring;[15,16] (2) an unsaturated Δ^8 or Δ^9 C ring with an exocyclic C11 methyl or hydroxy methyl; alternatively, a saturated C ring containing a 9-β-hydroxyl, 9-β-hydroxy methyl, or 9-keto functional group;[17-20] and (3) a C3 aliphatic side chain ranging from 3 to 7 carbons wherein heptyl analogues represent the optimum side chain length. In addition to the basic pharmacophore, substitution of the C3 side chain with 1′,1′-dimethyl, 1′,2′-dimethyl, and 1′,1′-ditholane generally enhances the activity of the CCBs.[21–26]

The understanding of the interplay between the pharmacophoric elements of CCBs and the ligand binding pocket (LBP) have been significantly refined as a result of QSAR studies and site directed mutagenesis of the LBP. Computational studies have identified the requirement for a hydrogen bond donor/acceptor pair in the C1 region of CCBs,[17,27–29] a result proposed to correlate with an interaction of the C1 hydroxyl with a critical Lys192 in the CB1 receptor.[30,31] An additional donor/acceptor pair between Tyr275 and the CCBs containing a hydroxyl in the C9 region may be responsible for the increased CB1 affinity relative to Δ^9-THC.[32]

The intramolecular geometries of the C1 and C9 substituents are tightly defined by the rigid ring system of the CCBs, however QSAR studies indicate moderate to high conformational flexibility in the C3 side chains.[27,33–35] These studies clearly demonstrate the LBP of CB1 prefers a hydrophobic substituent at C3 but the requirement for conformational flexibility remains to be fully elucidated. Progress to this end has been reported in studies of a series of conformationally restricted Δ^8-THC side chain analogues incorporating methylene and methyne functionalities[35] and 1′-cyclopropyl analogues.[36] The study suggests that the side chain adopts an orthogonal geometry relative to the plane of the aromatic ring with the tail of the side chain folding into a hydrophobic pocket. Despite the incorporation of unsaturation into the side chains, considerable flexibility remains in this set of molecules. The inherent computational limitations in predicting the conformation of a flexible side chain, in the absence of X-ray crystallographic or high resolution NMR data, somewhat limits the ability to predict the preferred side chain geometry and LBP steric requirements of the CB receptors.

To better understand the conformational and steric requirements of the hydrophobic pocket of the LBP interacting with the C3 side chain of CCBs, we designed and synthesized a series of Δ^8-THC analogues restricted in both the orientation and flexibility of the side chain. In order to probe the size and depth of the pocket, cycloalkyl groups of 5, 6 and 7 carbons, that is, cyclic equivalents of highly active CCBs, were appended to the C1′ position to restrict the degrees of freedom within the side chain. The C1′ position was further substituted with either a 1′,1′-dimethyl or a 1′,1′-dithiolane functionality in an effort to bias the rotation about the C3-C1′ bond. In this study we report the binding affinities of these compounds with the CB1 and CB2 receptors as well as Δ^8-THC and 1′,1′-dithiolanepentyl Δ^8-THC. Furthermore, the results of 1D and 2D high field NMR studies and quantum mechanical calculations are reported as part of our effort to determine the geometries of the side chains relative to the aromatic ring and as such the SAR of the ligand binding pocket.

Results

Chemistry

The synthesis of the side chain modified analogues of Δ^8-THC was carried out by the acid catalyzed coupling of *cis*-Δ^2-*p*-menthene-1,8-diol with the appropriately substituted resorcinol.[33] The precursor resorcinols were synthesized as summarized in Scheme 1, by reacting 3,5-dimethoxybenzonitrile with the Grignard of the appropriate alkyl or cycloalkyl halide followed by HCl hydrolysis of the resulting imine to yield ketones **5–8**.[37] These ketones were then reacted with either ethane-1,2-dithiol in the presence of $BF_3{\cdot}Et_2O$ to give the corresponding dithiolanes **9–12**[33] or reacted with dimethylzinc and $TiCl_4$ thus yielding the corresponding *gem*-dimethyl intermediates **13–15**.[37] Deprotection of the intermediate aryl ethers using BBr_3 at 0 °C for 12–16 h generated the 5-substituted resorcinols **16–22**. Reaction of the resorcinols with *cis*-Δ^2-*p*-menthene-1,8-diol, prepared from (+)-Δ^2-carene according to the method of Prasad and Dev,[38] in the presence of *p*-toluenesulphonic acid monohydrate gave the corresponding Δ^8-THC analogues **23–29**.

Receptor binding assays

Cell membranes from HEK293 cells transfected with the human CB1 cannabinoid receptor and membranes from CHO-K1 cells transfected with the human CB2 cannabinoid receptor were used in the receptor binding assays. Displacement of [^{3}H]CP 55,940 from the CB1 and CB2 receptor preparations by increasing concentrations of the Δ^8-THC analogues **23–29** and Δ^8-THC were used to determine the binding affinities of the conformationally biased probes (Table 1). The K_i values for Δ^8-THC at the hCB1 and hCB2 receptor were 28.5 nM and 25.0 nM, respectively (affinity ratio CB1/CB2 = 1.14), compared to a reported value of 47.6 nM for the rCB1 and 39.3 for the mCB2 (affinity ratio CB1/CB2 = 1.21).[39] The LBP probes exhibited a 3- to 143-fold enhancement in binding affinity to the receptor subtypes relative to Δ^8-THC. The *gem*-dimethyl analogues **27–29** and the pentyl dithiolane **23** possessed sub-nanomolar affinities for both the CB1 and CB2 receptors that are comparable to the highly potent 1′,1′-dimethylheptyl- Δ^8-THC (DMHT, $K_i = 0.77$ nM).[40] Within this group of compounds the 1′,1′-dimethylcyclopentyl, **27**, had the highest affinity for the CB1 receptor ($K_i = 0.34$ nM) while the 1′,1′-dimethylcycloheptyl, **29**, exhibited greater affinity for the CB2 receptor ($K_i = 0.22$ nM). Despite the relatively high affinity, none of the compounds showed significant selectivity between receptor subtypes.

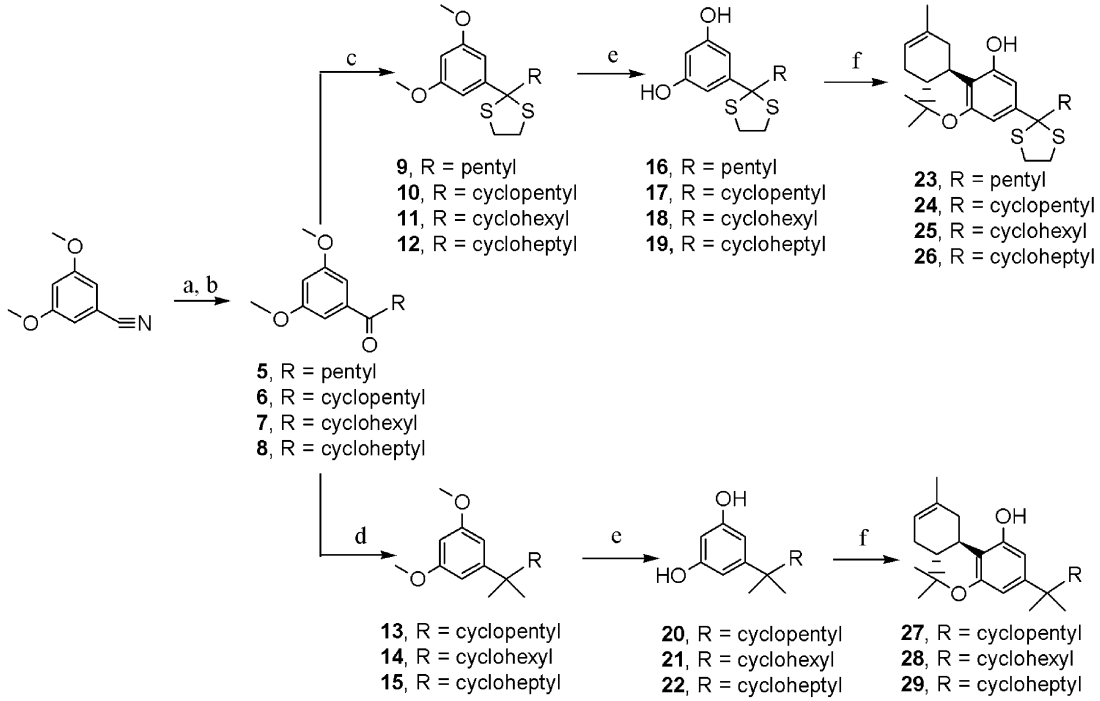

Scheme 1. Reagents and conditions: (a) RMgBr, THF, reflux, 3 h; (b) 6N HCl, reflux; (c)BF_3–Et_2O, ethanedithiol, CH_2Cl_2, rt, overnight; (d) Me_2Zn, $TiCl_4$; (e) BBr_3, 0 °C; (f) *cis*-Menth-2-ene-1,8,diol, *p*-TsOH, benzene, 80 °C.

The substitution of the 1′,1′-dimethyl for the 1′,1′-dithiolane group unexpectedly resulted in decreased affinity for both the CB1 and CB2 receptors. This series did not parallel the affinities observed within the synthesized 1′,1,-dimethyl analogues and had distinctly higher K_i′s than 1′,1′-dithiolaneheptyl- Δ^8-THC (DTHT, $K_i = 0.32$ nM).[33] Within this series of compounds the carbon equivalent of the later, **25**, had a K_i of 1.86 nM suggesting the structural requirements of the receptors are related to steric constraints. The 1′,1′-dithiolanepentyl analogue **23** had a 4.7-fold and 11 fold increased affinity for the CB1 and CB2 receptors, respectively, relative to the carbon equivalent **24**. These data combined with the 2- to 28-fold decrease in affinity of **24**–**26,** relative to **27**–**29**, for the CB1 suggest that this series may help define the steric limitations of the LBP. Furthermore, based on the steric requirements of the dithiolane series, modest receptor subtype selectivity is observed when considering the 1.76 nM K_i of **26** for the CB1 receptor and the 2.74 nM K_i of **24** for the CB2 receptor. The overall results of the receptor binding studies on both series suggest that we have developed Δ^8-THC analogues that will aid in the development of the SAR of the LBP with respect to the CCBs.

Table 1. Binding affinities of Δ^8-THC and analogues **23**–**29** for the CB1 and CB2 receptors

Compd	CB_1 K_i (nM)[a]	CB_2 K_i (nM)[a]	Ratio CB_1/CB_2
Δ^8-THC	28.5 (±3.3)	25.0 (±4.8)	1.14
23	0.85 (±0.02)	0.58 (±0.03)	1.47
24	9.49 (±2.42)	2.74 (±1.10)	3.46
25	1.86 (±0.71)	1.05 (±0.41)	1.77
26	1.76 (±0.56)	6.62 (±0.92)	0.27
27	0.34 (±0.04)	0.39 (±0.06)	0.84
28	0.57 (±0.05)	0.65 (±0.04)	0.87
29	0.94 (±0.05)	0.22 (±0.01)	4.65

[a]The K_i values for Δ^8-THC and the analogues were obtained from $n \geq 2$ independent experiments run in triplicate showing the standard error of the mean in parentheses.

NMR and molecular modeling studies

The binding affinities of the dimethyl-cycloalkyl analogues for both the CB1 and CB2 receptors are comparable to that of the highly potent 1′,1′-dimethylheptyl THC (DMHT, $K_i = 0.77$nM) analogue. Molecular modeling analysis of these compounds shows that the linear dimension of DMHT is 7.72 Å compared to 4.55 Å for **28**, which is the cyclic carbon equivalent of DMHT. The difference of 3.17 Å in the linear length of the side chain suggested that there is a region in the LBP that accommodates the C3 substituent which can be characterized as a hydrophobic ellipsoid. It remains unclear if this is the same pocket that accommodates the side chain of linear analogues; however, the potential existence of an ellipsoid pocket made it important to characterize the relative geometry of the cyclic side chain with respect to the tricyclic ring system. One facet of this effort utilized 1D and 2D high field NMR spectroscopy to assess the relative side chain geometries; furthermore, extensive NOESY studies on **28** were conducted to obtain distance constraints for use in molecular modeling.

The chemical shifts of the constituent protons in analogues **23**–**29** were first assigned utilizing 1D, *g*HSQC, *g*HMBC, and *g*COSY experiments. Based on these assignments the relative spatial orientations of the protons were examined via 2D NOESY experiments. In all the derivatives a network of NOEs interconnecting the

tricyclic ring system protons were observed. The NOESY experiments on **27–29** show strong NOEs between the H2 and H4 protons of the aromatic ring and the dimethyl and cycloalkyl methyne protons (Fig. 1); furthermore, the methylene units alpha to the methyne of the cycloalkyls show medium NOEs to the aromatic protons. A similar pattern is observed with respect to the dithiolane probes **24–26** with the notable addition of two weak NOEs to one each of the dithiolane methylenes. The presence of these NOEs to the dithiolane methylene and the multiplet between 3.07–3.33 ppm, that is, diastereotopic protons (Fig. 2), observed for these protons suggests that the ring flexibility is restrained and as such the protons reside in unique regions of the aromatic shielding/desheilding cone. The NOE patterns and intensities observed for the LBP probes suggest a conformational bias of the C3 side chains.

A qualitative analysis of the NOE intensities combined with model building suggest that cycloalkyl functionalities extend away from the aromatic ring and do not fold over the ring in solution, that is, the distinct absence of NOEs between the H4′-H6′and H2/H4 protons (Fig. 1). To more accurately examine the relative ring orientation, NOESY experiments using mixing times from 300–700 ms over 100 ms intervals were carried out on **28**. This analogue was selected for investigation because it is the carbon equivalent of DMHT. The spectra exhibited 41 clearly resolved NOEs with a subpopulation of 8 signals arising from the cyclohexyl to the H2 and H4 protons. Integration of those non-overlapping unambiguously assigned peaks utilizing TRIPOS TRIAD software followed by constraint generation using MARDIGRAS resulted in a web of 26 distance constraints (Fig. 3).[41] Utilizing these constraints, the model was subjected to 1 ns of constrained molecular dynamics to determine the populations of torsional conformers associated with the experimental NMR data. The resulting conformations show a single constraint violation between the cyclohexane methyne and one of the aromatic protons, most likely due to interconversion between the 41 and 319 degree torsional angles for the C3–C1′–C2′–C3′ (τ_2) bond, representing the two torsional populations observed in the simulated annealing studies (Fig. 4). Multiple torsional driving utilizing grid searches failed to predict these geometries suggesting that electronic effects were responsible for the conformations observed in the NMR studies. Therefore, quantum mechanical calculations were employed to examine the electronic effects driving the structural bias.

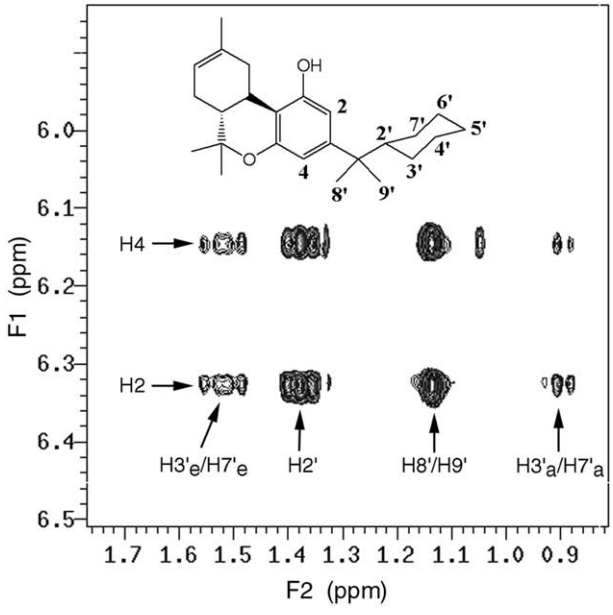

Figure 1. Partial 2D NOESY spectra (300 ms mixing time) of **28** showing the NOEs between the aromatic protons H2/H4 and the methylene, H3′/H7′, and methyne proton, H2′, on the cyclohexyl ring.

Quantum mechanical calculations

It seemed reasonable to assume that the *gem*-dimethyl would adopt a conformer that would maximize the interaction between the conformationally biased side chain and the aromatic ring. However, the conformation of the cyclohexyl analogue **28** predicted by NMR and molecular dynamics could not be explained based on molecular mechanics calculations, that is, electrostatic and steric analysis. To address this issue, semi-empirical and density functional theory (DFT) calculations have been employed to critically evaluate the potential conformers and determine the importance of electronic contributions in the experimental results.

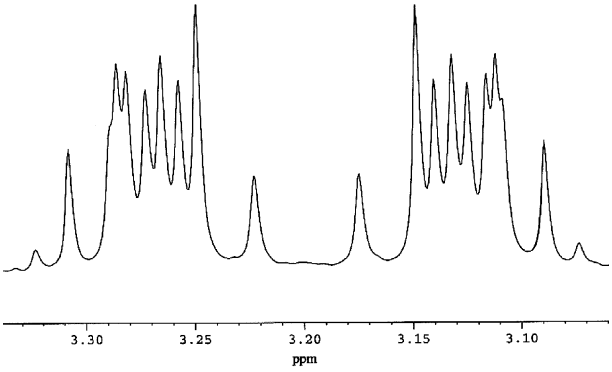

Figure 2. Partial 1D NMR spectra of **25** showing the diastereotopic methylene protons of the dithiolane group.

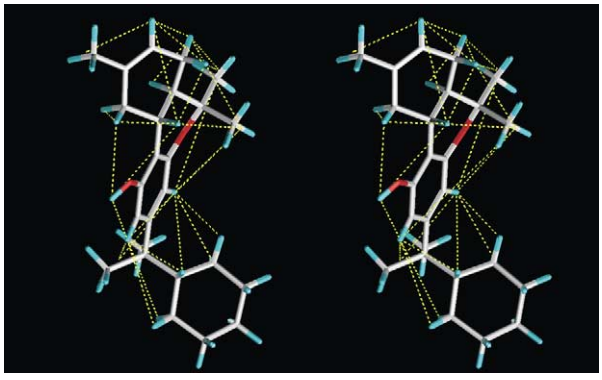

Figure 3. Stereoscopic view of **28** showing the NOE constraints (dashed yellow lines) derived from the 2D NOESY experiments. Carbon atoms are shown in white, hydrogen atoms in cyan and oxygen atoms are red.

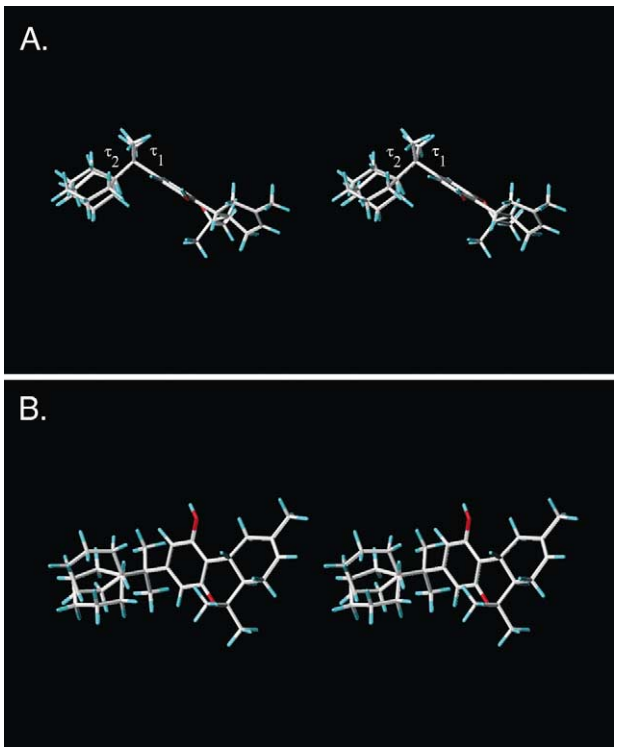

Figure 4. Stereoscopic views of **28** showing the two cyclohexyl side-chain conformations identified in the molecular dynamics studies. Panel A shows the side chain geometry looking down the plane of the tricycle ring system and panel B is a view looking into the plane of the ring sysem. Carbon atoms are shown in white, hydrogen atoms in cyan and oxygen atoms are red.

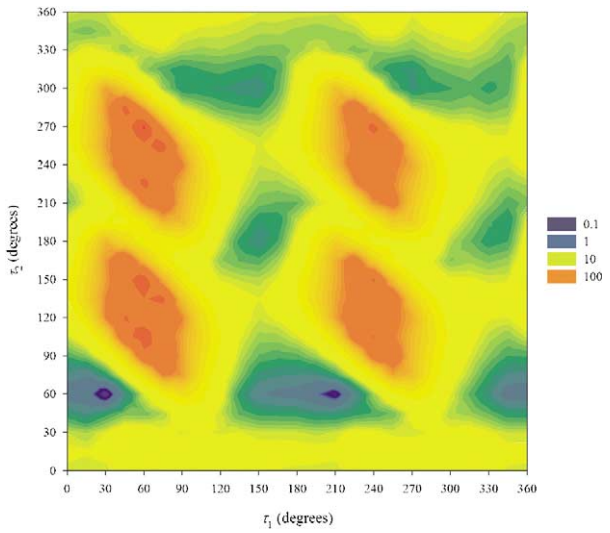

Figure 5. Calculated PM3 potential energy surface of **28** as a function of torsional parameters $\tau_1$and τ_2. Energies are the calculated heat of formation in Hartrees. The AM1 potential energy surface (omitted) has identical qualitative features.

Geometry optimizations were performed using both the AM1 and PM3 semi-empirical parameterizations with the GAMESS computational chemistry package.[42] The stationary points were confirmed by calculating the Hessian at the optimized geometries. Using these optimized structures, the potential energy surface (PES) was calculated using both AM1 and PM3 as a function of the rotations around the C2–C3–C1′–C2′ (τ_1) and C3–C1′–C2′–C3′ (τ_2) bonds with all other geometric parameters held constant. Both semi-empirical potential energy surfaces show that there is relatively free rotation about the τ_1 and τ_2 bonds (Fig. 5). More pronounced 'ridges' on the PM3 surface result from more diffuse electron densities produced with the PM3 parameterization relative to AM1. The four large peaks in the PES are the result of near collisions between a methylene hydrogen on the cyclohexyl group and the C2 hydrogen of the THC moiety. The most severe of these collisions arise from a 1.03 Å separation between two hydrogen atoms.

There are six regions on the PES that represent local minima for analogue **28** which can be designated by ordered pairs of angles according to (τ_1, τ_2) as A(141,56), B(259,301), C(270,180), D(323,56), E(40,305), and F(108,190). Geometry optimizations at the PM3 level were performed to identify the local minima nearest to each of these points followed by a DFT energy calculation using the B3LYP functional and a 6-31G(*p,d*) basis set. In addition, the associated conformer obtained by an 180° rotation about the τ_1 bond was identified in the same manner (designated A′, B′, etc.). The range of values for the τ_2 dihedral is 56 to 305 degrees for the quantum mechanical calculations whereas the dynamics study predicted a range of 41 to 319. The relative energies for the six lowest energy conformations at the B3LYP/6-31G(*p,d*) level[43,44] are given in Table 2. Note that the largest energy difference between these structures is only 0.6 kcal/mol (roughly 8.8 milliHartrees) suggesting that all conformers are thermally accessible. Observed deviations between the molecular modeling results and the quantum mechanical results are small enough, that is, within 10%, to justify agreement between the two methods.

However, the NMR data suggests that there is a preferred conformation in the solvent phase, suggesting that the electronic contributions may be important. Figure 6, panel B shows the HOMO orbital diagram (from the B3LYP/6-31G(*p,d*) calculations) for the *gem*-dimethyl analogue **28**. In this conformation there is an orbital lobe associated with the hydrogen atom bonded to the C3′ carbon atom. The shape of this lobe suggests an anti-bonding sigma orbital and indicates a repulsive interaction between the hydrogen atom and the electron

Table 2. Relative energy differences (kcal/mol) between the six lowest energies on the potential energy surface for the gem-dimethyl analogue (**26**)

Conformation[a]	ΔE (kcal/mol)
F′ (101,60)	0.55
B (259,301)	0.52
A (141,56)	0.38
A′ (124,193)	0.09
F (108,190)	0.05
D′ (302,193)	0.00

[a]Numbers in parenthesis are the ordered pairs of angles (τ_1,τ_2).

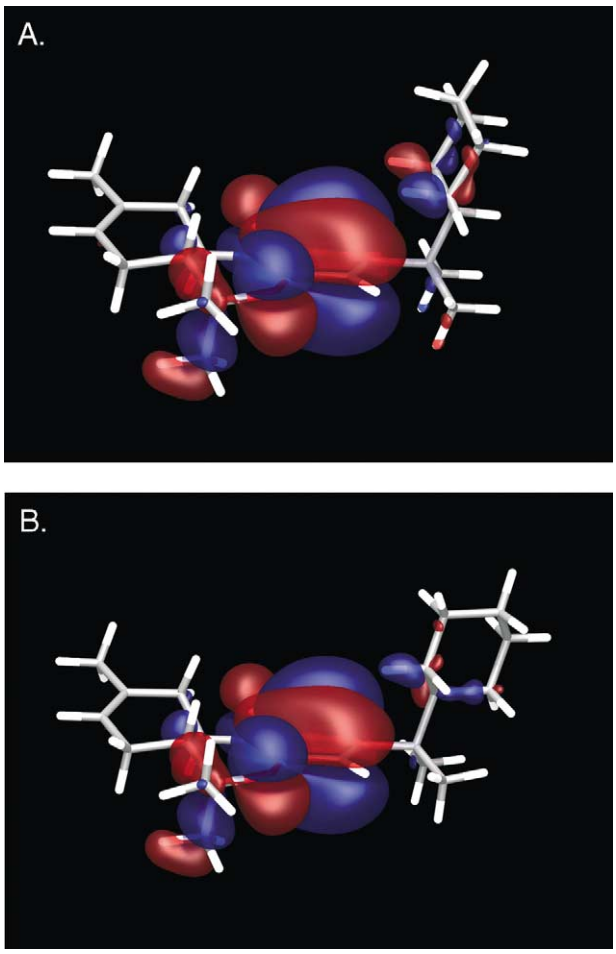

Figure 6. Orbital diagrams of the calculated HOMO at the B3LYP/6-31G(*p,d*) level of theory. The shape of the orbital lobes centered on the cyclohexyl hydrogen atoms is suggestive of antibonding σ orbitals associated with hydrogen 1*s* atomic orbitals. Part A demonstrates a repulsive interaction between two of the cyclohexyl hydrogen atoms and the aromatic orbital lobes on ring A whereas Part B shows only one such interaction. There is noticeable distortion of the orbital lobes associated with ring A, which supports a significant repulsion between the cyclohexyl hydrogen atoms and the electron density associated with the aromatic ring.

density of the aromatic ring. An examination of the shape of the orbital lobes associated with the aromatic ring shows a deformation associated with this hydrogen interaction. Figure 6, panel A shows the HOMO orbital diagram for the same compound after a rotation of 180 degrees about the τ_2 angle and a subsequent reoptimization as described previously. In this case we notice two such repulsions between the aromatic ring and the nearest hydrogen atom causing an increase in energy of 0.28 kcal/mol. Although small, this energy could be sufficient to cause conformational preference in the solvent phase. This feature can be observed because of the quality of the B3LYP functional and the presence of diffuse functions in the 6-31G(*p,d*) basis set. By comparison with the experimental results we can surmise that the bias in the NMR spectrum is the result of electronic interactions between the aromatic ring and the terminal hydrogens of the cyclohexyl group, favoring conformations that minimize the number of such repulsions.

Discussion

The objective of this research was to design and synthesize novel Δ^8-THC analogues as probes of the side chain LBP pocket of the CB1 and CB2 receptors. It was hypothesized that cycloalkyl side chains that contain identical carbon numbers as known high affinity ligands but that have reduced linear dimensions may provide insight into the side chain pocket geometry. To this end seven novel Δ^8-THC analogues were synthesized and tested for binding affinity to the human CB1 and CB2 receptors. The dimethylcycloalkyl analogues **27**–**29** had K_i values (0.34 to 0.94 nM) comparable to those of highly potent CB1 analogues such as DHMT (0.77 nM) and 1′,2′-dimethylheptyls (0.46–0.84 nM). In contrast, the introduction of the 1′,1′-dithiolane ring to the cycloalkyl analogues decreased receptor binding as compared to the dimethyl series. The notable exception is **23** wherein a 33- and 47-fold increase in binding to the CB1 and CB2 receptors, respectively, is observed relative to Δ^8-THC. Caution must also be exercised when comparing receptor binding data from different species and that obtained from different receptor preparations; however, the affinity ratio for the hCB1 to rCB1 found in our assays was 1.67 while the ratio for the hCB2 to mCB2 was 1.57. Factoring in this ratio our compounds remain comparable to other known high affinity CB ligands.

The most significant difference in CB1 affinity occurs within the cyclopentyl and pentyl compounds **23, 24,** and **27**. Interestingly, **23** and **27** have high affinities for the CB1 receptor in contrast to **24** that has an 11- to 28-fold decrease in CB1 affinity. The physical basis for the increased K_i for **24** may reflect the limited rotation of τ_1 due the dithiolane ring that thus prevents the cyclopentyl group from optimizing interactions with the receptor. This limitation to rotation about τ_1 and τ_2 is not predicted based on the NMR and quantum mechanical calculations on **28** thus suggesting that **27** can adopt geometries that maximize receptor interactions. In particular, despite the conformational flexibility about τ_2, the steric bulk of the cyclohexyl group prevents free rotation about τ_1. Analogue **23** is not restricted by the steric constraints associated with the cyclic analogues and as such can adopt receptor favorable conformations. In contrast to the affinities of **24**–**26** for the CB1 receptor the dithiolane ring does not appear to be as well tolerated by the CB2 receptor, that is, a 7- and 33-fold decrease in affinity for **24** and **26**. This combined with the data for CB1 affinity suggests that the LBP side chain requirements between the receptor subtypes are sensitive to steric bulk.

By far the most important finding of this study is that cycloalkyl side chains bind to both the CB1 and CB2 receptors with affinities comparable to the linear chain-Δ^8-THC analogues, for example, DMHT. An analysis of the maximum linear dimensions for the cyclic side chain analogues range from 3.90 Å for **27** to 4.99 Å for **29** compared to 7.72 Å for DMHT. These distances combined with the receptor binding data suggest the existence of an ellipsoidal hydrophobic pocket that may or may not represent the pocket occupied by the linear

side chain analogues. The orientation of the C3 side chain in solution with respect to the tricyclic ring system projects 124 degrees from the plane of the aromatic ring base on NMR and quantum mechanical calculations. The results of our studies provide insights into the solution conformations of the Δ^8-THC analogues, which may reflect the LBP spatial constraints of these CB ligands. The orientation of the side C3 side chain in the LBP cannot be conclusively defined since ligands do bind receptors in conformations different from solution or crystal structures. Furthermore, the analogue affinities cannot be correlated with ligand efficacy since a number of high affinity ligands exhibit poor efficacy in functional assays.[45] Functional assays on this series of compounds will ultimately permit us to refine the structural requirements of the LBD of the CB receptors and properties of these analogues.

Conclusion

We have synthesized restricted side chain analogues of Δ^8-THC as probes of the LBP of the CB1 and CB2 receptors. Analogues **27–29** have affinities for the CB1 and CB2 receptors comparable to known high affinity CCB ligands while the dithiolane derivatives **24** and **26** have reduced affinity. The receptor binding data suggest that the side chain binding pocket for this series of compounds can be characterized as a hydrophobic ellipsoid. Though the functional potency need not correlate with binding affinities, the K_i values give an indication of part of the receptor structure and provide for improvement on the CCB structure to produce higher affinity analogues. The determination of the functional activity of the reported compounds combined with SAR studies on the CCBs should provide invaluable insights into the development of this class of CB receptor analogues. Furthermore, the aforementioned studies may help clarify if the ellipsoid pocket is the same pocket occupied by the linear side chain CB analogues.

Experimental

All chemicals and reagents were purchased from Sigma-Aldrich or Fisher Scientific Inc. Anhydrous solvents were prepared by distillation over sodium metal or calcium hydride just prior to use. All reactions were carried out under dry conditions and under an argon atmosphere. Silica Gel 60, 200–425 mesh was used for flash chromatography. ^{1}H NMRs, ^{13}C NMRs and 2D spectra were obtained on a Varian 500 Inova MHz NMR and were consistent with the assigned structures. All NMR were recorded in $CDCl_3$ unless otherwise specified. Routine mass spectra were determined on a Bruker ESQUIRE Ion Trap LC/MS(n) system while HRMS were measured at the Mass Spectrometry Center, University of Tennessee, Knoxville. IR spectra were measured on a Perkin–Elmer Model 1605 FT infrared spectrophotometer. Thin layer chromatography was performed on silica gel plates (Merck TLC plates, silica gel 60, F_{254})

1-(3,5-Dimethoxy-phenyl)-pentan-1-one (5). To Mg turnings (1.12 g, 46.7 mmol), dried in an oven for 1 h, and dry THF (32 mL) was added 1-butylbromide (4.46 g, 32.5 mmol) and allowed to react at reflux for half an hour. After formation of the Grignard, 3,5-dimethoxybenzonitrile (4 g, 24.5 mmol) was added and the mixture was refluxed for 4 h. The reaction was cooled with ice for 15 min followed by the slow addition of 40 mL of 6N HCl and then the mixture was refluxed for 16 h. The THF was removed and the residue dissolved in EtOAc (60 mL) and 6N HCl (15 mL). The layers were separated, the aqueous layer extracted with EtOAc (4×20 mL). The combined EtOAc extracts were extracted and washed with saturated $NaHCO_3$, water and brine. After drying the organic phase was concentrated and the residue resolved on silica gel eluting with EtOAc/hexanes (5:25), to yield 3.52 g (64.7%) of compound **5** as a white solid. R_f = 0.43 (Hexane/ethyl acetate 9:1); IR (KBr pellet) 2956, 1601, 1206, 1067, 755 cm^{-1}; ^{1}H NMR δ 7.09 (d, J = 2.31 Hz, 2H), 6.64 (t, J = 2.31 Hz, 1H), 3.84 (s, 6H), 2.92 (t, J = 7.4 Hz, 2H), 1.71 (q, J = 7.71 Hz, 2H), 1.40 (s, J = 7.71 Hz, 2H), 0.95 (t, J = 7.32 Hz, 3H); ^{13}C NMR δ 200.51, 161.10, 139.33, 106.17, 105.29, 55.83, 38.70, 26.84, 22.71, 14.17; MS: (ESI, Pos.) m/z 245 ([M$^+$23]$^+$).

Utilizing the appropriate alkylbromides the following compounds were similarly prepared from 3,5-dimethoxybenzonitrile.

Cyclopentyl-(3,5-dimethoxy-phenyl)-methanone (6). Yield 2.90 g (50.2%) as a clear oil. R_f = 0.58 (hexane/ethyl acetate 9:1); IR (KBr neat) 2956, 1604, 1204, 1067, 755 cm^{-1}; ^{1}H NMR δ 7.11 (d, J = 2.31 Hz, 2H), 6.63 (t, J = 2.29 Hz, 1H), 3.83 (s, 6H), 3.70–3.60 (m, 1H), 1.95–1.87 (m, 4H), 1.75–1.59 (m, 4H); ^{13}C NMR δ 202.71, 161.06, 139.23, 106.57, 105.11, 55.80, 46.72, 30.35, 26.54; MS: (ESI, Pos.) m/z 257 ([M$^+$23]$^+$).

Cyclohexyl-(3,5-dimethoxy-phenyl)-methanone (7). Yield 19.3 g (63.3%) as a clear oil. R_f = 0.43 (hexane/ethyl acetate 9:1); IR (KBr neat) 2936, 1594, 1200, 1059, 734 cm^{-1}; ^{1}H NMR δ 7.08 (d, J = 2.4 Hz, 2H), 6.63 (t, J = 2.25 Hz, 1H), 3.83 (s, 6H), 3.24–3.14 (m, 1H), 2.05–1.71 (m, 5H), 1.54–1.19 (m, 5H); ^{13}C NMR δ 203.73, 161.12, 138.61, 106.35, 104.92, 55.77, 45.99, 30.39, 29.73, 27.12, 26.17, 26.05; MS: (ESI, Pos.) m/z 271 ([M$^+$23]$^+$).

Cycloheptyl-(3,5-dimethoxy-phenyl)-methanone (8). Yield 11.0 g (45.6%) as a clear oil. R_f = 0.58 (hexane/ethyl acetate 9:1); IR (KBr neat), 2941, 1592, 1201, 1063, 757 cm^{-1}; ^{1}H NMR δ 7.07 (d, J = 2.4 Hz, 2H), 6.64 (t, J = 2.4 Hz, 1H), 3.84 (s, 6H), 3.40–3.32 (m, 1H), 1.96–1.52 (m, 12H). ^{13}C NMR δ 204.16, 161.12, 138.72, 106.40, 104.96, 55.80, 46.99, 46.66, 31.59, 31.13, 28.55, 28.36, 28.08, 27.04; MS: (ESI, Pos.) m/z 285 ([M$^+$23]$^+$).

2-Butyl-2-(3,5-dimethoxy-phenyl)-[1,3]dithiolane (9). To a stirred solution of **5** (3.52 g, 15.9 mmol) in anhydrous CH_2Cl_2 (58 mL); was added BF_3–Et_2O (0.58 mL, 4.8 mmol) and ethane-1,2-dithiol (2.71 g, 28.8 mmol) and stirred at room temperature for 16 h. The organic phase

was then extracted with 10% NaOH (20 mL) followed by water and brine. The organic phase was dried, concentrated and the residue resolved over silica gel eluting with EtOAc/hexanes (5:10) to yield 4.50 g (95.2%) of **9** as a colorless oil. R_f = 0.51 (hexane/ethyl acetate 9:1); IR (neat) 2955, 1205, 1067 694 cm^{-1}; ^1H NMR δ 6.89 (d, J = 2.22 Hz, 2H), 6.34 (t, J = 2.21 Hz, 1H), 3.81 (s, 6H). 3.40–3.20 (m, 4H), 2.33 (t, J = 7.53 2H), 1.31–1.20 (m, 4H), 0.85 (t, J = 6.78 Hz, 3H). ^{13}C NMR δ 160.56, 148.04, 106.01, 98.74, 74.58, 55.60, 45.92, 39.33, 30.23, 23.03, 14.13; MS: (ESI, Pos.) m/z 299 (M^+).

Utilizing the appropriate arylketones the following dithiolanes were similarly prepared.

2-Cyclopentyl-2-(3,5-dimethoxy-phenyl)-[1,3]dithiolane (10). Yield 2.92 g (87%) as an oil. R_f = 0.52 (hexane/ethyl acetate 92:8); IR (neat) 2955, 1206, 1066, 694 cm^{-1}; ^1H NMR δ 6.98 (d, J = 2.19 Hz, 2H), 6.34 (t, J = 2.25 Hz, 1H), 3.80 (s, 6H), 3.35–3.09 (m, 4H), 2.82–2.71 (m, 1H), 1.80–1.43 (m, 8H). ^{13}C NMR δ 160.03, 149.37, 106.37, 98.35, 79.474, 55.35, 52.14, 38.79, 31.17, 25.73; MS: (ESI, Pos.) m/z 333 ($[M^+23]^+$).

2-Cyclohexyl-2-(3,5-dimethoxy-phenyl)-[1,3]dithiolane (11). Yield 16.8 g (89.6%) as an oil. R_f = 0.43 (hexane/ethyl acetate 92:8); IR (neat) 2930, 1198, 1062, 698 cm^{-1}; ^1H NMR δ 6.94 (d, J = 2.4 Hz, 2H), 6.33 (t, J = 2.25 Hz, 1H), 3.80 (s, 6H), 3.33–3.09 (m, 4H), 2.17–2.09 (m, 1H), 1.92–1.88 (m, 2H), 1.73–1.58 (m, 3H), 1.27–0.97 (m, 5H). ^{13}C NMR δ 160.20, 148.17, 107.00, 98.59, 80.97, 55.60, 50.71, 39.07, 31.18, 26.91, 26.35; MS: (ESI, Pos.) m/z 347 ($[M^+23]^+$).

2-Cycloheptyl-2-(3,5-dimethoxy-phenyl)-[1,3]dithiolane (12). Yield 3.60 g (79.2%) as an oil. R_f = 0.56 (hexane/ethyl acetate 92:8); IR (neat) 2925, 1206, 1067, 832, 693 cm^{-1}; ^1H NMR δ 6.94 (d, J = 2.4 Hz, 2H), 6.32 (t, J = 2.25 Hz, 1H), 3.80 (s, 6H), 3.31–3.10 (m, 4H), 2.40–2.32 (m, 1H), 1.96–1.30 (m, 12H). ^{13}C NMR δ 160.38, 148.94, 106.52, 98.48, 81.99, 70.21, 55.60, 51.27, 45.22, 39.34, 32.82, 29.80, 28.04, 27.77; MS: (ESI, Pos.) m/z 361 ($[M^+23]^+$).

61-(1-Cyclopentyl-1-methyl-ethyl)-3,5-dimethoxy-benzene (13). In a dry three-necked flask equipped with an addition funnel was added anhydrous CH_2Cl_2 (80 mL) and cooled to −40 °C. A 1 M solution of $TiCl_4$ in CH_2Cl_2 (102 mL, 102 mmol) was transferred to the addition funnel and added slowly to the cold CH_2Cl_2 solution maintaining a temperature of −40 °C. The solution was cooled to −50 °C and via the addition funnel a 2 M solution of dimethylzinc in toluene (51 mL, 102 mmol) was added as rapidly as possible, maintaining the temperature between −40 and −50 °C. Upon completion of the addition, the viscous red solution was stirred vigorously for 10 min, after which a solution of **6** (4.01 g, 17.1 mmol) in dry CH_2Cl_2 (20 mL) was added rapidly maintaining the temperature between −45 and −35 °C. The temperature was then allowed to rise slowly to −10 °C over 2 h with constant stirring. The mixture was poured into ice/water (200 mL) and the aqueous layer was extracted with CH_2Cl_2 (4×50 mL). The combined organic extracts were washed with saturated $NaHCO_3$, water and brine, dried and concentrated. The residue was resolved over silica gel EtOAc/hexanes (1:9) to yield 2.75 g (65.0%) of **13** as a colorless oil. R_f = 0.50 (hexane/ethyl acetate 95:5); IR (neat) 2955, 1457, 1422, 1205, 1067, 831 cm^{-1}; ^1H NMR δ 6.53 (d, J = 2.4 Hz, 2H), 6.30 (t, J = 2.25, 1H), 3.79 (s, 6H), 1.55–1.38 (m, 7H), 1.25 (s, 6H), 1.21–1.15 (m, 2H); ^{13}C NMR δ 160.50, 153.36, 105.30, 96.76, 55.45, 51.80, 39.90, 27.94, 25.97, 25.82; MS: (ESI, Pos.) m/z 249 ($[M+H]^+$).

Utilizing the appropriate arylketones the following 1′,1′-*gem*-dimethyl compounds were similarly prepared.

1-(1-Cyclohexyl-1-methyl-ethyl)-3,5-dimethoxy-benzene (14). Yield 3.69 g (70.3%) as an oil. R_f = 0.55 (hexane/ethyl acetate 95:5); IR (neat) 2932, 1457, 1422, 1208, 1066, 702 cm^{-1}; ^1H NMR δ 6.48 (d, J = 2.4 Hz, 2H), 6.35 (t, J = 2.1 Hz, 1H), 3.80 (s, 6H), 1.72–1.55 (m, 6H), 1.45–1.39 (m, 1H), 1.21 (s, 6H), 1.18–1.05 (m, 2H), 0.97–0.85 (m, 2H); ^{13}C NMR δ 160.52, 153.48, 105.35, 96.64, 55.44, 49.28, 41.06, 28.18, 27.44, 26.96, 25.50; MS: (ESI, Pos.) m/z 263 ($[M+H]^+$).

1-(1-Cycloheptane-1-methyl-ethyl)-3,5-dimethoxy-benzene (15). Yield 3.61 g (72.3%) as an oil. R_f = 0.50 (hexane/ethyl acetate 95:5) IR (neat) 2934, 1455, 1422, 1206, 1067, 701 cm^{-1}; ^1H NMR δ 6.50 (d, J = 2.5 Hz, 2H), 6.29 (t, J = 2.25 Hz, 1H), 3.80 (s, 6H), 1.73–1.69 (m, 1H), 1.65–1.50 (m, H), 1.48–1.38 (m, H), 1.37–1.28 (m, H), 1.18 (s, 6H); ^{13}C NMR δ 160.33, 153.83, 104.94, 96.41, 55.21, 49.21, 42.03, 29.52, 28.06, 27.95, 25.19; MS: (ESI, Pos.) m/z 277 ($[M+H]^+$).

5-(2-Butyl-[1,3]dithiolan-2-yl)-benzene-1,3-diol (16). Boron tribromide (32.9 mL of 1M soln, 32.9 mmol) was added to a solution of **9** (4.51 g, 3.23 mmol) in CH_2Cl_2 (546 mL) under argon at −78 °C. The reaction temperature was then raised slowly to 0 °C over a period of 3 h. Stirring was continued at 0 °C for 12–14 h or until completion of reaction. Unreacted boron tribromide was destroyed by adding methanol, solvent removed and the residual oil diluted with diethyl ether. The organic phase was washed with saturated $NaHCO_3$, water and brine, dried and concentrated. The residue was resolved over silica gel eluting with diethylether/hexanes (4:6) to yield 0.675 g (74.1%) of **16** as a waxy solid. R_f = 0.28 (hexane/ethyl acetate 8:2) ^1H NMR δ 6.79 (d, J = 2.5 Hz, 2H), 6.23 (t, J = 2H, 1H), 5.30 (br s, 2H), 3.38–3.19 (m, 4H), 2.25 (t, J = 9.75 Hz, 2H), 1.29–1.18 (m, 4H), 0.83 (t, J = 7 Hz, 3H); ^{13}C NMR δ 156.24, 148.45, 107.23, 101.50, 73.90, 45.50, 39.01, 29.96, 22.74, 13.86; MS: (ESI, Neg.) m/z 269 ($[M-H]^-$).

Utilizing the appropriate dimethoxy-aryl-3′-substituted precursors the following resorcinol compounds were similarly prepared.

5-(2-Cyclopentyl-[1,3]dithiolan-2-yl)-benzene-1,3-diol (17). Yield 0.67 g (74.1%) as a waxy solid. R_f = 0.28 (hexane/ethyl acetate 8:2); ^1H NMR δ 6.89 (d, J = 2.4 Hz, 2H), 6.23 (t, J = 2.1 Hz, 1H), 5.68 (br s, 2H), 3.34–3.07 (m,

4H), 2.78–2.67 (m, 1H), 1.71–1.38 (m, 8H); ^{13}C NMR δ 156.26, 150.31, 108.13, 101.59, 79.28, 52.27, 39.02, 31.39, 25.94; MS: (ESI, Pos.) m/z 305 ($[M+23]^+$).

5-(2-Cyclohexyl-[1,3]dithiolan-2-yl)-benzene-1,3-diol (18). Yield 0.853 g (62.2%) as a waxy solid. R_f = 0.27 (hexane/ethyl acetate 8:2); ^{1}H NMR δ 6.78 (d, J = 0.9 Hz, 2H), 6.19 (t, J = 1.95 Hz, 1H), 4.14 (br s, 2H), 3.32–3.07 (m, 4H), 2.15–2.06 (m, 1H), 1.96–1.58 (m, 4H), 1.19–1.00 (m, 4H); ^{13}C NMR δ 156.95, 147.94, 107.39, 101.12, 80.58, 60.83, 50.56, 38.82, 30.92, 26.77, 26.24, 21.08, 14.17; MS: (ESI, Neg.) m/z 295 ($[M-H]^-$).

5-(2-Cycloheptyl-[1,3]dithiolan-2-yl)-benzene-1,3-diol (19). Yield 0.582 g (41.5%) as a waxy solid. R_f = 0.28 (hexane/ethyl acetate 8:2); ^{1}H NMR δ 6.85 (d, J = 2.4 Hz, 2H), 6.22 (t, J = 2.25 Hz, 1H), 5.16 (br s, 2H), 3.31–3.07 (m, 4H), 2.35–2.28 (m, 1H), 1.97–1.29 (m, 12H); ^{13}C NMR δ 156.07, 149.33, 107.65, 101.25, 50.92, 39.00, 32.55, 27.70, 27.43; MS: (ESI, Pos.) m/z 333 ($[M+23]^+$).

5-(1-Cyclopentyl-1-methyl-ethyl)-benzene-1,3-diol (20). Yield 1.29 g (72.9%) as a viscous oil. R_f = 0.28 (hexane:diethyl ether 6:4); ^{1}H NMR δ 6.44 (d, J = 2.1 Hz, 2H), 6.20 (t, J = 2.1 Hz, 1H), 5.70 (br s, 2H), 2.02–1.98 (m, 1H), 1.57–1.35 (m, 6H), 1.18 (s, 6H); ^{13}C NMR δ 156.22, 154.66, 105.10, 99.83, 53.24, 50.33, 36.21, 24.99, 24.75; MS: (ESI, Neg.) m/z 219 ($[M-H]^-$).

5-(1-Cyclohexyl-1-methyl-ethyl)-benzene-1,3-diol (21). Yield 1.11 g (61.9%) as a viscous oil. R_f = 0.28 (hexane:diethyl ether 6:4); ^{1}H NMR δ 6.38 (d, J = 2 Hz, 2H), 6.17 (t, J = 2.25 Hz, 1H), 4.82 (br s, 2H), 1.71–1.68 (m, 2H), 1.63–1.60 (m, 1H), 1.53–1.51 (m, 2H), 1.42–1.36 (m, 1H), 1.17 (s, 6H), 1.16–1.03(m, 3H), 0.94–0.86 (m, 2H); ^{13}C NMR δ 156.32, 154.45, 106.56, 100.02, 49.21, 40.85, 28.12, 27.39, 26.91, 25.39, 14.40; MS: (ESI, Neg.) m/z 233 ($[M-H]^-$).

5-(1-Cycloheptyl-1-methyl-ethyl)-benzene-1,3-diol (22). Yield 0.442 g (24.7%) as a viscous oil. R_f = 0.26 (hexane:diethyl ether 6:4); ^{1}H NMR δ 6.40 (d, J = 2 Hz, 2H), 6.17 (t, J = 2 Hz, 1H), 4.74 (br s, 2H), 1.68–1.50 (m, 7H), 1.48–1.39 (m, 2H), 1.35–1.25 (m, 2H), 1.15 (s, 6H), 1.14–1.08 (m, 2H); ^{13}C NMR δ 156.15, 154.78, 106.13, 99.74, 49.22, 41.79, 29.46, 28.01, 27.88, 25.06; MS: (ESI, Neg.) m/z 247 ($[M-H]^-$).

3-(2-Butyl-[1,3]dithiolan-2-yl)-6,6,9-trimethyl-6a,7,10,10a-tetrahydro-6H-benzo[*c*]chromen-1-ol (23). To a solution of resorcinol **16** (650 mg, 2.4 mmol) in dry benzene (20 mL) was added *cis*-Menth-2-ene-1,8-diol (408 mg, 2.4 mmol) followed by the addition of *p*-toluenesulfonic acid monohydrate (19 mg, 0.099 mmol). The reaction mixture was stirred at 80 °C for 4 h. The reaction mixture was cooled and diluted with ether and washed well with saturated $NaHCO_3$, water and brine. After drying it was concentrated and the residue resolved on silica gel (1.9×25 cm), eluting with 3% diethylether–petroleum ether to yield 254 mg (26.3%) of **23** as a light yellow, waxy solid. R_f = 0.22 (petroleum ether/diethyl ether 9:1) ^{1}H NMR δ 6.77 (d, J = 2 Hz, 1H), 6.63 (d, J = 1.5 Hz, 1H), 5.44 (d, J = 4 Hz, 1H), 4.82 (s, 1H), 3.37–3.24 (m, 4H), 3.22–3.18 (m, 1H), 2.73–2.68 (m, 1H), 2.31–2.27 (m, 2H), 2.17–2.18 (m, 1H), 1.86–1.79 (m, 3H), 1.71 (s, 3H), 1.40 (s, 3H), 1.29–1.23 (m, 6H), 1.12 (s, 3H), 0.86–0.84 (m, 3H); ^{13}C NMR δ 154.81, 154.65, 144.23, 134.95, 119.53, 112.11, 109.55, 106.69, 77.17, 73.98, 45.87, 44.97, 39.40, 37.11, 36.03, 31.83, 30.18, 28.09, 27.81, 23.73, 23.04, 18.80, 14.17; HRMS (FAB), m/z, calcd for $C_{23}H_{32}O_2S_2$, 404.1844, experimental 404.1844.

The synthesis of the 3′-substituted $^8\Delta$-THC analogues was carried out using the appropriately substituted rescorcinol analogues.

3-(2-Cyclopentyl-[1,3]dithiolan-2-yl)-6,6,9-trimethyl-6a,7,10,10a-tetrahydro-6H-benzo[*c*]chromen-1-ol (24). Yield 55 mg (14.6%) as a light yellow, waxy solid. R_f = 0.22 (petroleum ether/diethyl ether 9:1) ^{1}H NMR δ 6.86 (d, J = 1.5 Hz, 1H), 6.70 (d, J = 2 Hz, 1H), 5.43 (d, J = 4 Hz, 1H), 4.76 (br s, 1H), 3.33–3.12 (m, 5H), 2.77–2.66 (m, 1H), 2.15–2.12 (m, 1H), 1.88–1.78 (m, 3H), 1.70 (s, 3H), 1.68–1.67 (m, 2H), 1.60–1.59 (m, 3H), 1.53–1.42 (m, 5H), 1.38 (s, 3H), 1.10 (s, 3H); ^{13}C NMR δ 154.55, 154.33, 146.82, 134.95, 119.53, 111.90, 110.12, 107.31, 79.00, 52.40, 44.98, 39.12, 36.06, 31.83, 31.41, 31.34, 28.08, 27.80, 25.91, 23.71, 18.77; HRMS (FAB), m/z, calcd for $C_{24}H_{32}O_2S_2$, 416.1844, experimental 416.1841.

3-(2-Cyclohexyl-[1,3]dithiolan-2-yl)-6,6,9-trimethyl-6a,7,10,10a-tetrahydro-6H-benzo[*c*]chromen-1-ol (25). Yield 193 mg (22.2%) as a light yellow solid. R_f = 0.22 (petroleum ether/diethyl ether 9:1) ^{1}H NMR δ 6.81 (d, J = 2 Hz, 1H), 6.65 (d, J = 2 Hz, 1H), 5.44 (d, J = 5 Hz, 1H), 4.79 (br s, 1H), 3.28–3.10 (m, 5H), 2.72–2.66 (m, 1H), 2.16–2.06 (m, 2H), 1.93–1.79 (m, 5H), 1.72–1.67 (m, 1H), 1.70 (s, 3H), 1.61–1.58 (m, 1H), 1.29–1.02 (m, 6H), 1.38 (s, 3H), 1.11 (s, 3H); ^{13}C NMR δ 154.48, 154.25, 145.36, 134.97, 119.54, 111.94, 110.44, 107.62, 80.35, 77.11, 66.14, 50.61, 44.99, 39.14, 36.07, 31.85, 31.07, 31.00, 28.10, 27.83, 26.88, 26.36, 23.74, 18.81, 15.50, 11.94; HRMS (FAB), m/z, calcd for $C_{25}H_{34}O_2S_2$, 430.2000, experimental 430.2000.

3-(2-Cycloheptyl-[1,3]dithiolan-2-yl)-6,6,9-trimethyl-6a,7,10,10a-tetrahydro-6H-benzo[*c*]chromen-1-ol (26). Yield 61 mg (14.2%) as a light yellow solid. R_f = 0.22 (petroleum ether/diethyl ether 9:1) ^{1}H NMR δ 6.82 (d, J = 1.5 Hz, 1H), 6.67 (d, J = 1.5 Hz, 1H), 5.426 (d, J = 4.5 Hz, 1H), 4.88 (br s, 1H), 3.28–3.11 (m, 5H), 2.72–2.66 (m, 1H), 2.33–2.28 (m, 1H), 2.16–2.13 (m, 1H), 1.93–1.79 (m, 7H), 1.70 (s, 3H), 1.39 (s, 3H), 1.11 (s, 3H), 1.93–1.28 (m, 8H); ^{13}C NMR δ 154.32, 154.18, 145.80, 134.69, 119.25, 111.59, 109.66, 106.87, 81.16, 76.85, 50.93, 44.67, 39.06, 35.78, 32.54, 32.47, 31.57, 27.78, 27.71, 27.54, 27.48, 23.46, 18.52; HRMS (FAB), m/z, calcd for $C_{26}H_{36}O_2S_2$, 444.2157, experimental 444.2170.

3-(1-Cyclopentyl-1-methyl-ethyl)-6,6,9-trimethyl-6a,7,10,10a-tetrahydro-6H-benzo[*c*]chromen-1-ol (27). Yield 334 mg (41.6%) as a light yellow solid. R_f = 0.32 (petroleum ether/diethyl ether 95:5); ^{1}H NMR δ 6.42 (d,

$J=1$ Hz, 1H), 6.26 (d, $J=2$ Hz, 1H), 5.43 (d, $J=5$ Hz, 1H), 4.66 (br s, 1H), 3.21–3.17 (m, 1H), 2.72–2.67 (m, 1H), 2.16–2.13 (m, 1H), 2.06–1.99 (m, 1H), 1.94–1.76 (m, 6H), 1.70 (s, 3H), 1.39 (s, 3H), 1.22–1.13 (m, 2H), 1.11 (s, 3H), 1.18 (s, 6H); ^{13}C NMR δ 154.8, 154.45, 150.68, 135.00, 119.58, 110.38, 108.60, 106.03, 76.90, 51.77, 45.11, 39.22, 36.25, 31.75, 28.13, 27.90, 27.86, 25.85, 25.76, 23.74, 18.76; HRMS (FAB), *m*/*z*, calcd for $C_{24}H_{34}O_2$, 354.2558, experimental 354.2566.

3 - (1 - Cyclohexyl - 1 - methyl - ethyl) - 6,6,9 - trimethyl-6a,7,10,10a-tetrahydro-6H-benzo[*c*]chromen-1-ol (28). Yield 298 mg (37.9%) as a light yellow solid. $R_f=0.33$ (petroleum ether/diethyl ether 95:5) ^{1}H NMR δ 6.37 (d, $J=2$ Hz 1H), 6.22 (d, $J=1.5$ Hz, 1H), 5.43 (d, $J=5$ Hz, 1H), 4.65(br s, 1H), 3.21–3.17 (m, 1H), 2.72–2.67 (m, 1H), 2.18–2.13 (m, 1H), 1.91–1.77 (m, 3H), 1.71(s, 3H), 1.67–1.67 (m, 2H), 1.61–1.50 (m, 4H), 1.39 (s, 3H), 1.41–1.36 (m, 1H), 1.16 (s, 3H), 1.15 (s, 3H), 1.10–1.03 (m, 3H), 0.92–0.75 (m, 2H); ^{13}C NMR δ 154.32, 154.23, 150.54, 134.76, 119.34, 110.08, 108.44, 105.80, 76.66, 48.84, 44.87, 40.155, 36.03, 31.51, 27.89, 27.63, 27.18, 26.72, 25.26, 24.93, 23.50, 18.53; HRMS (FAB), *m*/*z*, calcd for $C_{25}H_{36}O_2$, 368.2715, experimental 368.2715.

3 - (1 - Cycloheptyl - 1 - methyl - ethyl) - 6,6,9 - trimethyl-6a,7,10,10a-tetrahydro-6H-benzo[*c*]chromen-1-ol (29). Yield 341 mg (42.9%) as a light yellow waxy solid. $R_f=0.33$ (petroleum ether/diethyl ether 95:5) ^{1}H NMR δ 6.39 (d, $J=1.5$ Hz, 1H), 6.2 (d, $J=1.5$ Hz, 1H), 5.43 (d, $J=4.5$ Hz, 1H), 4.67 (br s, 1H), 3.21–3.17 (m, 1H), 2.72–2.67 (m, 1H), 2.16–2.10 (m, 1H), 1.91–1.79 (m, 3H), 1.70 (s, 3H), 1.67–1.51 (m, 8H), 1.47–1.41 (m, 2H), 1.38–1.26 (m, 3H), 1.14 (s, 6H), 1.11 (s, 3H), 1.12–1.07 (m, 1H); ^{13}C NMR δ 154.40, 154.29, 151.11, 134.77, 119.35, 110.05, 109.76, 108.31, 105.67, 76.65, 49.13, 44.89, 41.36, 36.05, 31.54, 29.48, 29.45, 28.16, 28.05, 27.94, 27.90, 27.87, 27.63, 25.15, 24.93, 23.50, 22.95, 18.52; HRMS (FAB), *m*/*z*, calcd for $C_{26}H_{38}O_2$, 382.2872, experimental 382.2878.

NMR studies and molecular modeling

All spectra were acquired at 23 °C and 500 MHz on a Varian Inova-500 spectrometer using a 5 mm HCN triple resonance probe. Both proton and carbon chemical shifts were referenced to the residual solvent peak of DMSO (2.49 ppm for proton and 40 ppm for carbon). For two-dimensional NOESY measurements, a total of 512 fids were recorded for the indirect dimension, with a 2 second recycle delay. The TRIAD NMR package within the Sybyl software was used for data processing and analysis. Peaks in the NOESY spectra were assigned and integrated using TRIAD standard functions. MARDIGRAS was then used to generate distance constraints for **28** using these peak integrals. Results from each of the five mixing times gave very similar distance constraints, hence each distance constraint was averaged over the five mixing times to get the final set of distance constraints for the molecule. The resulting constraints were then examined to ensure that the error in distances conformed to established errors for NOE constraints wherein; $x<2.5$ Å was +/− 0.1 Å; $x\leq 3.0$ Å was +/− 0.2 Å; $x\leq 3.5$ Å was +/− 0.3 Å; and $x\geq 3.5$ was +/− 0.4 Å.

A four-step simulated annealing using 1 fs time steps and the constraints generated by MARDIGRAS was performed on **28** as follows: (1) 1 ps dynamics at 300 K; (2) 1 ps heating to 500 K; (3) another 1 ps heating phase to 700 K; (4) a 1 ns equilibration to 500 K. Additional parameters included the Tripos force field with Gasteiger-Hückel charges, an 8 Å nonbonding cutoff, and distance dependent dielectric constant function. The experimentally obtained NOE distance constraints were applied during all steps of the dynamics runs, and the aromatic carbons were defined as aggregates to maintain the ring geometry. The molecular geometry was sampled at 1000 fs intervals during phase (1) of the dynamics runs and once during the heating and cooling periods. A total of 1007 conformations were collected for further analysis and these were subjected to twenty dynamics simulations each to obtain average conformations. These average conformations were then minimized with a gradient tolerance of 0.005 kcal·mol^{-1}· Å^{-1} without defined aggregates or experimental NOE distance constraints to obtain the final average conformations.

Quantum mechanical calculations

Quantum mechanical calculations were performed using the GAMESS computational chemistry package on a SGI Origin 2000 with 8 processors and 4GB of memory. Molecular orbital surfaces were calculated from the B3LYP/6-31G(*p,d*) results using a version of MOLDEN[46] modified at The University of Memphis. Potential energy surfaces were calculated using the AM1 and PM3 semi-empirical wavefunctions, as were the final geometries optimizations.

Receptor binding assays

Cell membranes from HEK293 cells transfected with the human CB1 receptor (Lot #1929, B_{max}: 1.7 pmol/mg protein, K_d for [^{3}H]CP 55,940 binding: 186 pM) and membranes from CHO-K1 cells transfected with the human CB2 receptor (Lot #1930, B_{max}: 3.3 pmol/mg protein, K_d for [^{3}H]CP 55,940 binding: 0.12 nM) were purchased from Perkin–Elmer Life Sciences, Inc. [^{3}H]CP 55,940 having a specific activity of 120 Ci/mmol was obtained from Perkin–Elmer Life Sciences, Inc. All other chemicals and reagents were obtained from Sigma-Aldrich. The assays were carried out in 96-well plates obtained from Millipore, Inc. fitted with glass fiber filters (hydrophilic, GFC filters) having a pore size of 1.2 μ. The filters were soaked with 0.05% polyethyleneimine solution and washed 5× with deionized water prior to carrying out the assays. The filtrations were carried out on a 96-well vacuum manifold (Millipore Inc.), the filters punched out with a pipette tip directly into scintillation vials at the end of the experiment and vials filled with 5 mL scintillation cocktail Ecolite (+) (Fisher Scientific). Counting was carried out on a Beckmann Scintillation Counter model LS6500.

Drug solutions were prepared in DMSO and the radioligand was dissolved in ethanol.

Incubation buffer: 50 mM TRIS–HCl, 5mM $MgCl_2$, 2.5 mM EDTA, 0.5 mg/mL fatty acid free bovine serum albumin, pH 7.4.

Binding protocol for the CB1 receptor: 8 μg of membranes (20 μL of a 1:8 dilution in incubation buffer) was incubated with 5 μL of drug solution (10^{-4} M to 10^{-12} M) and 5 μL of 5.4 nM [^{3}H]CP 55,940 in a total volume of 200 μL for 90 mins at 30 °C. Non-specific binding was determined using 10 μM WIN55,212-2 ($K_i = 4.4$ nM). The membranes were filtered and the filters washed 7× with 0.2 mL ice-cold incubation buffer and allowed to air dry under vacuum.

Binding protocol for the CB2 receptor: 15.3 μg of membranes (20 μL of a 1:20 dilution in incubation buffer) was incubated with 5 μL of drug solution (10^{-4}M to 10^{-12}M) and 5 μL of 10 nM [^{3}H]CP 55,940 in a total volume of 200 μL for 90 mins at 30 °C. Non-specific binding was determined using 10 μM WIN55,212-2 ($K_i = 4.4$ nM). The membranes were filtered and the filters washed 7× with 0.2 mL ice-cold incubation buffer and allowed to air dry under vacuum.

Data accumulation and statistical analysis: Varying concentrations of drug ranging from 10^{-4} M to 10^{-12} M were added in triplicate for each experiment and the individual molar IC_{50} values were determined using GraphPad Prism. The corresponding K_i values for each drug were determined utilizing the Cheng and Prusoff equation.[47] and final data are presented as $K_i \pm$S.E.M. of $n \geq 2$ experiments.

Acknowledgements

This research was supported by the College of Pharmacy, University of Tennessee Health Sciences Center. We would like to thank Dr. Henry Kurtz for his valuable insights and discussion on the quantum mechanical interpretations.

References and Notes

1. Gaoni, Y.; Mechoulam, R. *J. Am. Chem. Soc.* **1964**, *86*, 1646.
2. Gernard, C. M.; Mollereau, C.; Vassart, G.; Parmentier, M. *Biochem. J.* **1991**, *279*, 129.
3. Skaper, S. D.; Buriani, A.; Dal Toso, R.; Petrelli, L.; Romamello, S.; Facci, L.; Leon, A. *Proc. Natl. Acad. Sci. U.S.A.* **1996**, *93*, 3984.
4. Matsuda, L. A.; Lolait, S. J.; Brownstein, M. J.; Young, A. C.; Bonner, T. I. *Nature* **1990**, *346*, 61.
5. Munro, S.; Thomas, K. L.; Abu-Shaar, M. *Nature* **1993**, *365*, 61.
6. Di Marzo, V.; Goparaju, S. K.; Wang, L.; Liu, J.; Batkai, S.; Jarai, Z.; Fezza, F.; Miura, G. I.; Palmiter, R. D.; Sugiura, T.; Kunos, G. *Nature* **2001**, *410*, 822.
7. Parolaro, D.; Massi, P.; Rubino, T.; Monti, E. *Prostaglandins Leukot. Essent. Fatty Acids* **2002**, *66*, 319.
8. Palmer, S. L.; Thakur, G. A.; Makriyannis, A. *Chem. Phys. Lipids* **2002**, *121*, 3.
9. Porcella, A.; Maxia, C.; Gessa, G. L.; Pani, L. *Eur. J. Neurosci.* **2001**, *13*, 409.
10. Chien, F. Y.; Wang, R. F.; Mittag, T. W.; Podos, S. M. *Arch. Ophthalmol.* **2003**, *121*, 87.
11. Melvin, L. S.; Johnson, M. R.; Herbert, C. A.; Miline, G. M.; Weissmen, A. A. *J. Med. Chem.* **1984**, *27*, 67.
12. Lan, R.; Liu, Q.; Fan, P.; Lin, S.; Fernando, S. R.; McCallion, D.; Pertwee, R.; Makriyannis, A. *J. Med. Chem.* **1999**, *42*, 769.
13. D'Ambra, T. E.; Estep, K. G.; Bell, M. R.; Eissentat, M. A.; Josef, K. A.; Ward, S. J.; Haycock, D. A.; Baizman, E. R.; Casiano, F. M.; Beglin, N. C.; Chippari, S. M.; Grego, J. D.; Kullnig, R. K.; Daley, G. T. *J. Med. Chem.* **1992**, *35*, 124.
14. Seltzman, H. H. *Curr. Med.Chem.* **1999**, *6*, 685.
15. Razdan, R. K. *Pharmac. Rev.* **1986**, *38*, 75.
16. Uliss, D. B.; Dalzell, H. D.; Handrick, G. R.; Howes, J. F.; Razdan, R. K. *J. Med. Chem.* **1975**, *18*, 213.
17. Thomas, B. F.; Compton, D. R.; Martin, B. R.; Semus, S. F. *Mol. Pharmacol.* **1991**, *40*, 656.
18. Wilson, R. S.; May, E. L.; Martin, B. R.; Dewey, W. L. *J. Med. Chem.* **1976**, *19*, 1165.
19. Melvin, L. S.; Milne, G. M.; Johnson, M. R.; Subramaniam, B.; Wilken, G. H.; Howlett, A. C. *Mol. Pharmacol.* **1993**, *44*, 1008.
20. Mechoulam, R.; Feigenbaum, J. J.; Lander, N.; Segal, M.; Jarbe, T. U.; Hiltunen, A. J.; Consroe, P. *Experientia* **1988**, *44*, 762.
21. Huffman, J. W.; Lainton, J. A. H.; Banner, W. K.; Duncan, J. S. G.; Jordan, R. D.; Yu, S.; Dai, D.; Martin, B. R.; Wiley, J. L.; Compton, D. R. *Tetrahedron* **1997**, *53*, 1557.
22. Huffman, J. W.; Duncan, S. G.; Wiley, J. L.; Martin, B. R. *Bioorganic Med. Chem. Lett.* **1997**, *7*, 2799.
23. Guo, Y.; Abadji, V.; Morse, K. L.; Fournier, D. J.; Li, X.; Makriyannis, A. *J. Med. Chem.* **1994**, *37*, 3867.
24. Devane, W. A.; Breuer, A.; Sheskin, T.; Jarbe, T. U. C.; Eisen, M. S.; Mechoulam, R. *J. Med. Chem.* **1992**, *35*, 2065.
25. Tius, M. A.; Hill, W. A. G.; Zou, X. L.; Busch-Petersen, J.; Kawakami, J. K.; Femandez-Garcia, M. C.; Drake, D. J.; Abadji, V.; Makriyannis, A. *Life Sci.* **1995**, *56*, 2007.
26. Huffman, J. W.; Yu, S.; Showalter, V.; Abood, M. E.; Wiley, J. L.; Compton, D. R.; Martin, B. R.; Bramblett, R. D.; Reggio, P. H. *J. Med. Chem.* **1996**, *39*, 3875.
27. Schmetzer, S.; Greenidge, P.; Kovar, K. A.; Schulze-Alexandru, M.; Folkers, G. *J. Comp.-Aided Mol. Des.* **1997**, *11*, 278.
28. Reggio, P. H.; Greer, K. V.; Cox, S. M. *J. Med. Chem.* **1989**, *32*, 1630.
29. Johnson, M. R.; Melvin, L. S. *Cannabinoids as Therapeutic Agents*; CRC Press: Boca Raton, FL, 1986.
30. Song, Z. H.; Bonner, T. I. *Mol. Pharmacol.* **1996**, *49*, 891.
31. Chin, C.; Lucas-Lenard, J.; Abadji, V.; Kendall, D. A. *J. Neurochem.* **1998**, *70*, 280.
32. McAllister, S. D.; Tao, Q.; Barnett-Norris, J.; Buehner, K.; Hurst, D. P.; Guarnieri, F.; Reggio, P. H.; Nowell Harmon, K. W.; Cabral, G. A.; Abood, M. E. *Biochem. Pharmacol.* **2002**, *63*, 2121.
33. Papahatjis, D. P.; Kourouli, T.; Abadji, V.; Goutopoulos, A.; Makriyannis, A. A. *J. Med. Chem.* **1998**, *41*, 1195.
34. Ryan, W.; Singer, M.; Razdan, R. K.; Compton, D. R.; Martin, B. R. *Life Sci.* **1995**, *56*, 2013.
35. Keimowitz, A. R.; Martin, B. R.; Razdan, R. K.; Crocker, P. J.; Mascarella, S. W.; Thomas, B. F. *J. Med. Chem.* **2000**, *43*, 59.
36. Papahatjis, D. P.; Nikas, S. P.; Andreou, T.; Makriyannis, A. *Bioorg. Med. Chem. Lett.* **2002**, *12*, 3583.

37. Singer, M.; Ryan, W. J.; Saha, B.; Martin, B. R.; Razdan, R. K. *J. Med. Chem.* **1998**, *41*, 4400.
38. Prasad, R. S.; Dev, S. *Tetrahedron* **1976**, *32*, 1437.
39. Busch-Petersen, J.; Hill, W. A.; Fan, P.; Khanolkar, A.; Xie, X.-Q.; Tius, M. A.; Makriyannis, A. *J. Med. Chem.* **1996**, *39*, 3790.
40. Martin, B. R.; Compton, D. R.; Semus, S. F.; Lin, S.; MArciniak, G.; Grzybowska, J.; Charalambous, A.; Makriyannis, A. *Pharmacol. Biochem. Behav.* **1993**, *46*, 295.
41. SYBYL, version 6.8; Tripos, Inc.: St. Louis, MO, 2001.
42. Schmidt, M. W.; Baldridge, K. K.; Boatz, J. A.; Elbert, S. T.; Gordon, M. S.; Jensen, J. H.; Koseki, S.; Matsunaga, N.; Nguyen, K. A.; Su, S.; Windus, T. L.; Dupuis, M.; Montgomery, J. A. *J. Comput. Chem.* **1993**, *14*, 1347.
43. Hehre, W. J.; Ditchfield, R.; Pople, J. A. *J. Chem. Phys* **1972**, *56*, 2257.
44. Hariharan, P. C.; Pople, J. A. *Theoret. Chimica Acta* **1973**, *28*, 213.
45. Griffin, G.; Williams, S.; Aung, M. M.; Razdan, R. K.; Martin, B. R.; Abood, M. E. *Br. J. Pharmacol.* **2001**, *132*, 525.
46. Schaftenaar, G.; Noordik, J. H. *J. Comput.-Aided Mol. Design* **2000**, *14*, 123.
47. Cheng, Y.; Prusoff, W. H. *Biochem. Pharmacol.* **1973**, *22*, 3099.